Supporting Information for

One-step hexaplex immunoassays by on-line paper substrate based electrospray ionization mass spectrometry for combined cancer biomarker screening

Shuting Xu,[a,c] Mingxia Liu,[a] Jie Feng,[b] Guangtao Yan,[b] Yu Bai *[a] and Huwei Liu [a]

[a] Beijing National Laboratory for Molecular Sciences, Key Laboratory of Bioorganic Chemistry and Molecular Engineering of Ministry of Education, College of Chemistry and Molecular Engineering, Peking University, Beijing 100871, P. R. China. Tel: +86 10 6275 8198; E-mail: yu.bai@pku.edu.cn

[b] Medical Laboratory Center, Chinese People's Liberation Army General Hospital, Beijing 100853, P. R. China.

[c] Institute of Analytical Food Safety, School of Food Science and Technology, Jiangnan University, Wuxi 214122, P. R. China.

* Phone: +86-10-62758198 (Y. B.).

* E-mail: yu.bai@pku.edu.cn (Y. B.).

This supporting information included the synthesis of six rhodamine-based mass tags (RMTs), preparation and characterization of immune paper substrates and mass probes (MPs), details of the paper substrate-based electrospray ionization (PS-ESI) setup, details of immunoassay validation, and comparison of this method with other representative multiplexed immunoassays.

Synthesis of Six Rhodamine-based Mass Tags (RMTs).

Chemicals: 11-Mercapto-1-undecanol (97%), 4-dimethylaminopyridine (DMAP, AR), and N,N'-dicyclohexylcarbodiimide (DCC, 99%) were purchased from Aladdin Co., Ltd. (Shanghai, China). 3-(Piperidin-1-yl)phenol (97%) was purchased from Ark Pharm, Inc. (Chicago, US). 3-Diethylaminophenol (98%), 3-dimethylaminophenol (97%), rhodamine 6G (AR), rhodamine 110 (AR), rhodamine 101 inner salt (92%), 4-carboxybenzaldehyde (97%),and chloranil (99%) were purchased from J&K Scientific Ltd. (Beijing, China). 30% Hydrogen peroxide, p-toluenesulfonic acid monohydrate (AR), sodium acetate (AR), sodium hydroxide (AR), sodium sulfate anhydrous (AR), sodiumiodide (99%), sodium thiosulfate pentahydrate (AR), thionyl chloride (AR), hydrochloric acid (36%-38%) and sodium sulfate anhydrous (AR) were purchased from Sinopharm Chemical Reagent Co., Ltd. (Shanghai, China). Propionic acid (AR), N,N'-dimethylformamide (DMF, AR), pyridine (AR), ethyl acetate (AR), *n*-hexane (AR), dichloromethane (AR), chloroform (AR), and methanol (AR) were purchased from Xilong Chemical Co. Ltd. (Shantou, Guangdong, China). Purified water was from Hangzhou Wahaha Group (Hangzhou, China).

The synthesis of six RMTs referred to our previous work, the synthetic routes were shown in Figure S1 and described as follow:

11, 11'-disulfanediylbis(undecan-1-ol) (**b**): The 11-mercapto-1-undecanol (**a**, 1 mmol, 204.4 mg) was dissolved in 5 mL of ethyl acetate followed by the addition of 30% hydrogen peroxide (1 mmol, 110 μL) and the catalyst sodiumiodide (0.01 mmol, 2.5 mg). The reaction occurred under stirring at room temperature. After about 30 min, a saturated solution of sodium thiosulfate was added under stirring to make the solution color from yellow to white. The organic phase was extracted with ethyl acetate, washed with brine and dried over sodium sulfate anhydrous. The solvent was removed by a rotary evaporator to yield a white solid product **b** (200 mg).

Six carboxy-substituted rhodamine heads: The 3-diethylaminophenol (**c1**) (or dimethylaminophenol, **c2**, or 3-(Piperidin-1-yl)phenol, **c3**, 5 mmol) with the 4-carboxybenzaldehyde (**d**, 2.5 mmol, 375 mg) and *p*-toluenesulfonic acid monohydrate (0.4 mmol, 76 mg) were added to 25 mL propionic acid, and the mixture was stirred at 65 °C for 16 h. After cooling to room temperature, the mixture was poured into sodium acetate aqueous (3 mol/L, 100 mL). The resulting suspension was extracted with chloroform, and the combined organic extracts were dried over sodium sulfate anhydrous. After the solvent was evaporated by a rotary evaporator, the solid product was dissolved in a mixture of 30 mL methanol and 20 mL chloroform, followed by the addition of chloranil (1.2 mmol, 295 mg). The mixture was stirred for 2 h at room temperature, and then concentrated by rotary evaporation. The residue was purified by the column chromatography using a mixture eluent of chloroform/methanol. After concentration, the product **e1**, **e2** and **e3** were

obtained as purple crystal as the rhodamine heads of RMT443, RMT 387, and RMT467, respectively.

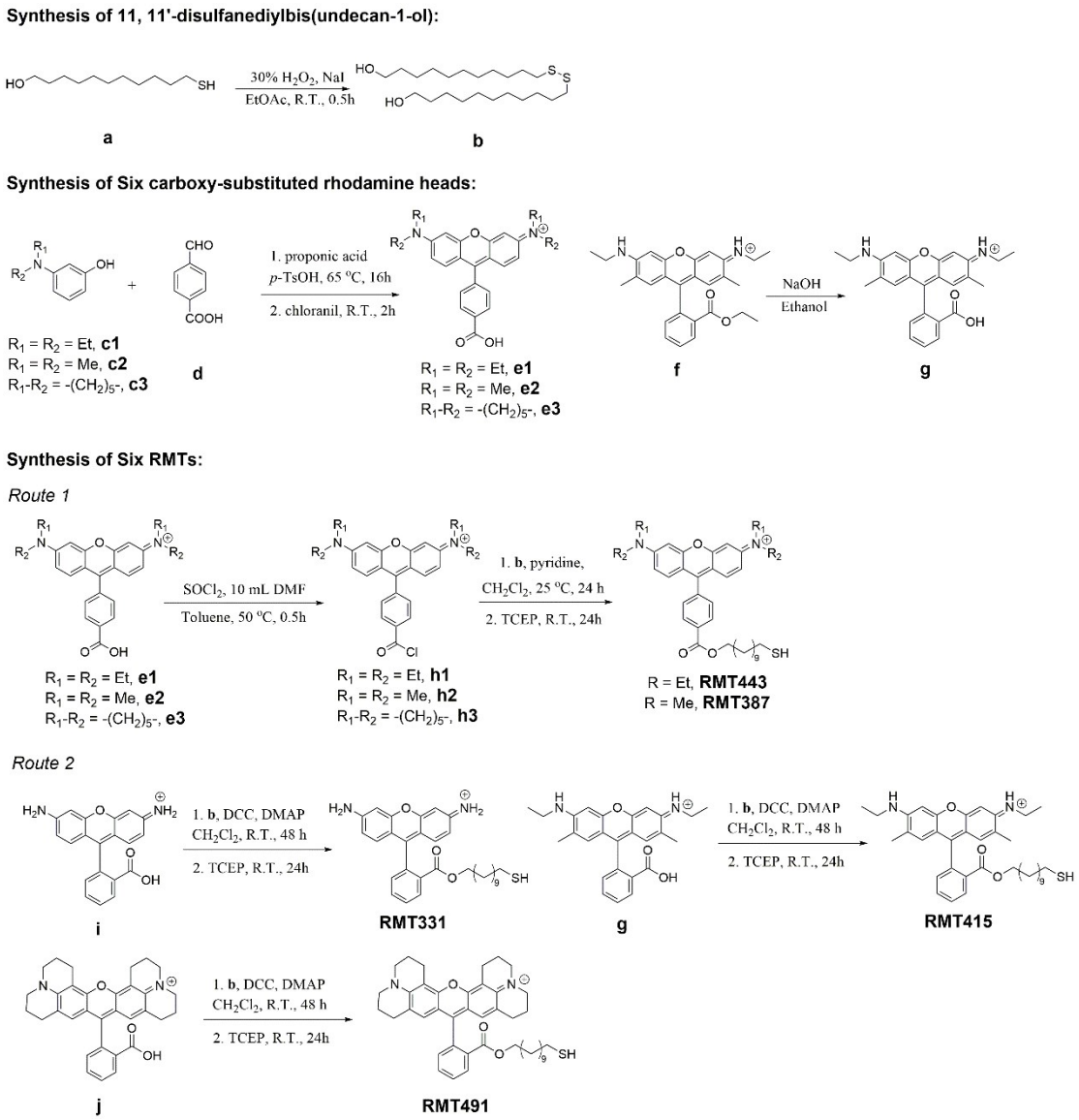

Fig. S1 Synthetic routes of rhodamine-based mass tags (RMT331, RMT387, RMT415, RMT443, RMT467, and RMT491).

The rhodamine head of RMT415 was obtained from the hydrolysate of rhodamine 6G. The rhodamine 6G (**f**, 2.26 mmol, 1 g) was dissolved in 10 mL ethanol, and 0.1 g sodium hydroxide (2.5 mmol) was added. The reaction was performed at 70 °C for 12 h. The ethanol was removed by evaporation, and 50 mL of ion exchanged water was added. 1 mol/L hydrochloric acid was added dropwise to adjust the pH value to 2, and the solution was stirred for 1 h. Hydrolysate of rhodamine 6G (**g**, 960 mg) was obtained after filtering the deposited crystal. The rhodamine head of RMT331 and RMT491 were commercial reagents rhodamine 110 and rhodamine 101 inner salt.

Target molecule RMTs: The esterification of rhodamine heads had two synthetic routes: *Route 1*: **e1**, or **e2** or **e3** (0.226 mmol) was dissolved in 7 mL of toluene, and 1 mL thionyl chloride was added dropwise under continuous stirring in ice bath, followed by the addition of catalyst 10 μL DMF. After the mixture was heated for 30 min at 60 °C, the solvent and thionyl chloride were removed by evaporation. The residue was washed by *n*-hexane for several times. The hexane was removed by evaporation to yield purple product **h1**, **h2**, and **h3** 4'-carbonyl chloride rhodamine. Then, product **b** (0.08 mmol, 33 mg) was mixed with **h1** (or **h2**, **h3**) in 4 mL anhydrous dichloromethane, followed by the addition of 14 μL pyridine (0.16 mmol). The mixture was stirred for 24 h at room temperature. After the evaporation of solvent, the residue was dissolved in 10 mL acetonitrile, and TCEP dissolved in 3 mL water were added. The mixture was stirred at room temperature for 24 h for the reduction of disulfide bonds. The residue was purified by the column chromatography using a mixture eluent of chloroform/methanol, and the target molecule **RMT443**, **RMT387** and **RMT467**. The final products were verified by high resolution mass spectrometry (HRMS): $[RMT443]^+$ calculated for $C_{39}H_{53}N_2O_3S^+$, 629.3771, found, 629.3771, MS/MS, 443.2327; $[RMT387]^+$ calculated for $C_{35}H_{45}N_2O_3S^+$, 573.3142, found, 573.3145, MS/MS, 387.1702; $[RMT467]^+$ calculated for $C_{41}H_{53}N_2O_3S^+$, 653.3771, found, 653.3771, MS/MS, 467.2327.

Route 2: **i**, or **g**, or **j** (0.24 mmol), product **b** (0.12 mmol, 48 mg), and DMAP (0.04 mmol, 5 mg) was dissolved in 7 mL of anhydrous dichloromethane, followed by the addition of DCC (0.36 mmol, 74 mg) dissolved in 3 mL anhydrous dichloromethane under continuous stirring in ice bath. The mixture was stirred under nitrogen at room temperature for 48 h. Then, 10 mL acetonitrile and TCEP (0.36 mmol, 100 mg) dissolved in 3 mL water were added, and the mixture was stirred at room temperature for 24 h. The concentrated residue was purified by the column chromatography using eluent of chloroform/methanol. After concentration, the product target molecule **RMT331**, **RMT415**, and **RMT491** were obtained. The final products were verified by high resolution mass spectrometry (HRMS): $[RMT415]^+$ calculated for $C_{37}H_{49}N_2O_3S^+$, 601.3457, found, 601.3458, MS/MS, 415.2015; $[RMT331]^+$ calculated for $C_{31}H_{37}N_2O_3S^+$, 517.2519, found, 517.2519, MS/MS, 331.1075; $[RMT491]^+$ calculated for $C_{43}H_{53}N_2O_3S^+$, 677.3770, found, 677.3771, MS/MS, 491.2327.

Six Target Proteins and Specific Antibodies.

Table S1. List of six target protein cancer biomarkers and their specific antibody pairs.

Protein cancer biomarkers		Antibody pairs		
Cancer antigen 15-3 (CA15-3)	Fitzgerald, Cat#30-1066	**Capture antibody**	Mouse monoclonal CA 15-3 antibody 1 (anti-CA15-3-1)	Fitzgerald, Cat#10-1145
		Detection antibody	Mouse monoclonal CA 15-3 antibody 2 (anti-CA15-3-2)	Fitzgerald, Cat#10-1144
Cancer antigen 19-9 (CA19-9)	Fitzgerald, Cat#30C-CP9063S	**Capture antibody**	Monoclonal CA 19-9 antibody 1 (anti-CA19-9-1)	Fitzgerald, Cat#10-CA19B
		Detection antibody	Mouse monoclonal CA 19-9 antibody 2 (anti-CA19-9-2)	Fitzgerald, Cat#10-CA19A
Carcinoma embryonic antigen (CEA)	Fitzgerald, Cat#30-AC30	**Capture antibody**	Mouse monoclonal CEA antibody 1 (anti-CEA-1)	Fitzgerald, Cat#10-C10DT
		Detection antibody	Mouse monoclonal CEA antibody 2 (anti-CEA-2)	Fitzgerald, Cat#10-C10ET
Cancer antigen 125 (CA125)	Fitzgerald, Cat#30C-CP1062	**Capture antibody**	Mouse monoclonal CA125 antibody 1 (anti-CA125-1)	Novus, Cat # NB120-10032
		Detection antibody	Mouse monoclonal CA125 antibody 2 (anti-CA125-2)	Novus, Cat#NB600-1468
Human epididymis protein 4 (HE4)	Fitzgerald, Cat#30-1338	**Capture antibody**	Mouse monoclonal HE4 antibody 1 (anti-HE4-1)	Fitzgerald, Cat#10-2460
		Detection antibody	Mouse monoclonal HE4 antibody 2 (anti-HE4-2)	Fitzgerald, Cat#10-2459
Alpha fetoprotein (AFP)	Fitzgerald, Cat#30-1029	**Capture antibody**	Mouse monoclonal AFP antibody 1 (anti-AFP-1)	Fitzgerald, Cat#10-2357
		Detection antibody	Mouse monoclonal AFP antibody 2 (anti-AFP-2)	Fitzgerald, Cat#10-2457

Other Chemicals and Materials for Immune Preparation and Detection.

Hydrogen tetrachloroaurate (III) hydrate was purchased from Beijing Chemical Works (Beijing, China). Potassium periodate (KIO_4, 99%), 2,4-dinitrophenylhydrazine (2,4-DNP, AR), sulfuric acid (AR), glycerol (AR), trisodium citrate dihydrate (AR) and potassium carbonate (K_2CO_3, AR) were purchased from Sinopharm Chemical Reagent Co., Ltd. (Shanghai, China). Tris(2-carboxyethyl)phosphine hydrochloride (TCEP, 98%), 4-(2-hydroxyethyl)-1-piperazineethanesulfonic acid (HEPES, AR), methanol (HPLC grade), 4, 7, 10, 13, 16, 19, 22, 25, 32, 35, 38, 41, 44, 47, 50, 53-hexadecaoxa-28, 29 dithiahexapentacontanedioic acid di-N-succinimidyl ester (NHS-PEG-S-S-PEG-NHS), crystal violet (CV, AR), immunoglobulin G (IgG) from rat serum, and bovine serum albumin (BSA) were purchased from Sigma-Aldrich (Shanghai, China). Goat anti-rat IgG and horse radish peroxidase (HRP)-conjugated goat anti-rat IgG were purchased from Shenggong Bioengineering Ltd. Company (Shanghai, China). 3,3',5,5'-tetramethylbenzidine (TMB) substrate chromogenic kit was purchased from Yuanye Bio-Technology Co., Ltd (Shanghai, China). Buffers used in our study were as follows: phosphate buffered saline (PBS, 10 mM, pH 7.4, containing 138 mmol/L NaCl, 2.7 mmol/L KCl), tris-HCl buffer (25 mmol/L, pH 7.4, containing 100 mmol/L NaCl, 5 mmol/L $MgCl_2$), and HEPES buffer (10 mmol/L, pH 7.5, containing 137 mmol/L NaCl). Purified water was produced by Hangzhou Wahaha Group (Hangzhou, China).

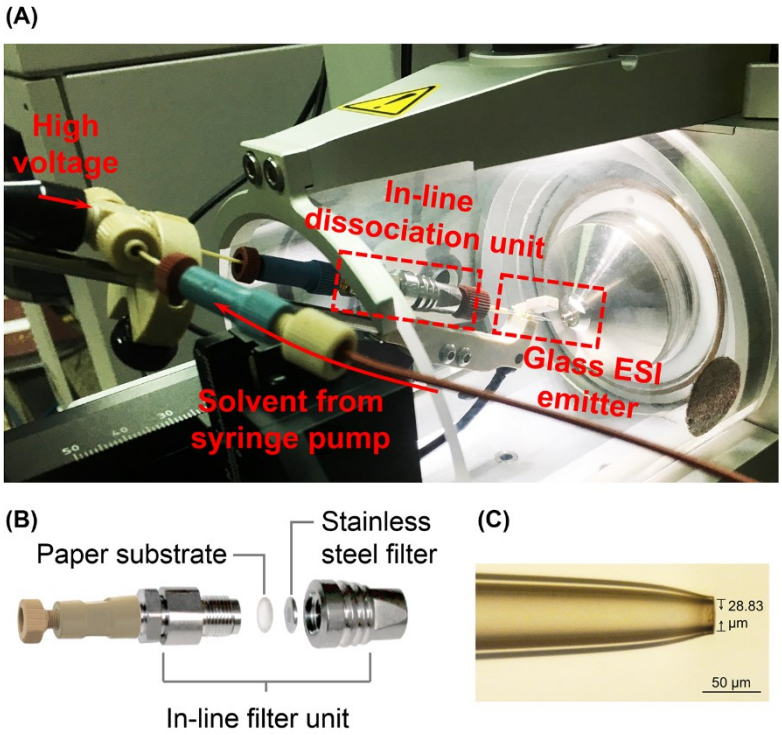

Fig. S2 (A) Photo of the paper substrate-based electrospray ionization setup (PS-ESI), containing a refitted in-line filter unit, home-made glass ESI emitter, cross joint for applied voltage and solvent supplied by syringe pump. (B) Components of the refitted in-line filter unit. (C) Micrograph of the glass electrospray emitters with a tip of about 30 µm.

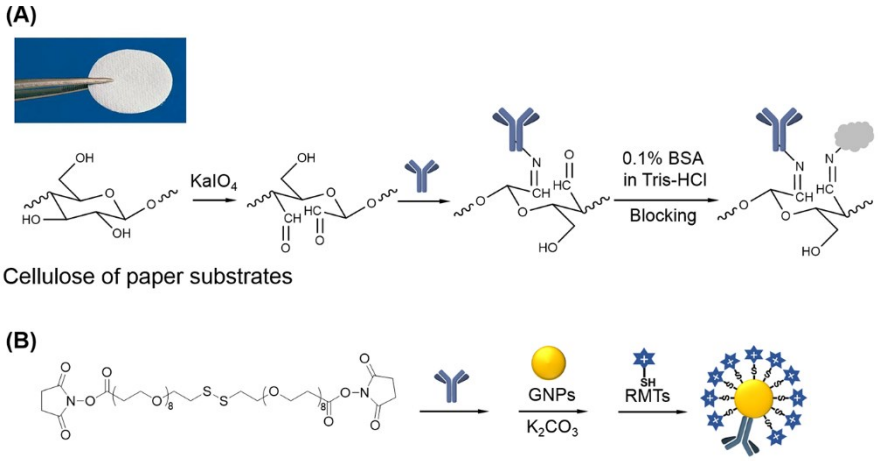

Fig. S3 (A) Route of capture antibody modification on paper substrates: oxidation of cellulose of paper substrates, covalent linkage of capture antibodies on oxidized paper substrates, and blocking of residual aldehyde groups on paper substrates. (B) Preparation route of mass probes (MPs): detection antibody linkage with thiol end groups, modified antibodies self-assembling on gold nanoparticles (GNPs), and RMTs self-assembling on GNPs.

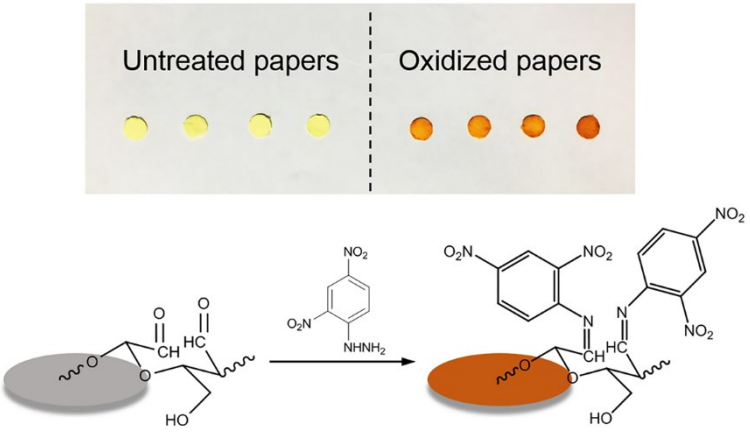

Fig. S4 2,4-dinitrophenylhydrazine (2,4-DNP) color reactions with aldehyde-functionalization paper substrates and untreated papers: the aldehyde-functionalization paper substrates presenting obvious orange and the untreated papers only remaining a slight yellow.

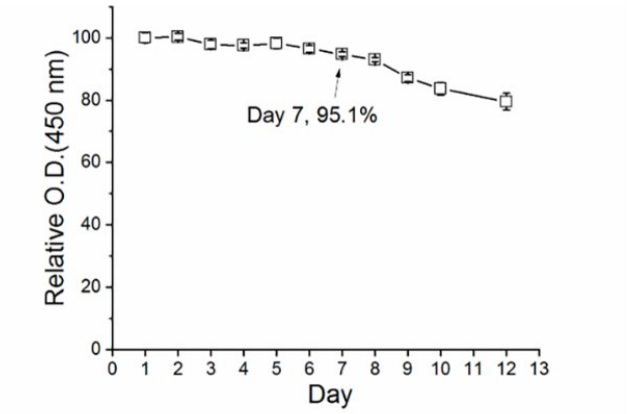

Fig. S5 The protein activity of HRP-conjugated anti-IgG modified substrates kept in PBS for more than a week.

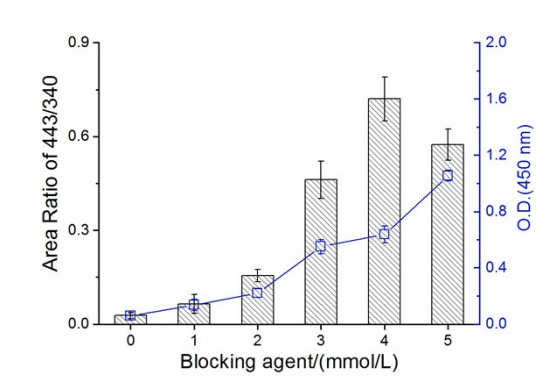

Fig. S6 The optimization of blocking agent (11-mercaptoundecyl)hexa(ethyleneglycol) (MUDOL) on GNPs, using both O.D. 450 nm values and MS signals of RMT443 fragment (m/z = 443.2) and IS (m/z = 340.2) for evaluation, the minimal non-specific signals appearing only without the addition of MUDOL.

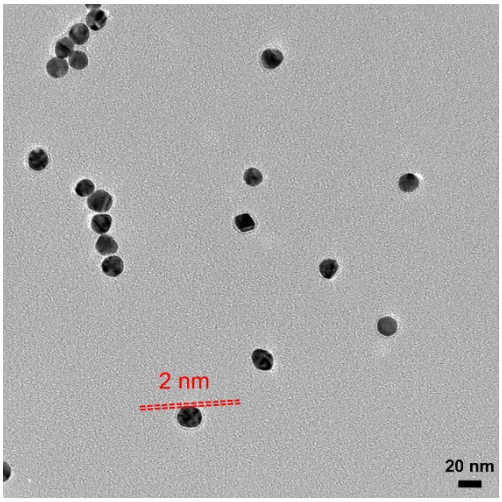

Fig. S7 Transmission electron microscopy (TEM) image of antibodies and RMT443 modified GNP probes, suggesting the spherical and monodispersed particles with about 20 nm in diameter and a modified corona of 2 nm thickness.

Table S2. Identification of dissociated mass tag derivatives of RMT443 based on the parent ions and tandem MS ions.

	Formula	Parent ions m/z	Tandem MS ions m/z
1	$C_{78}H_{104}N_4O_6S_2^{2+}$	628.5	443.3, 430.3, 398.3
2	$C_{39}H_{53}N_2O_3S^+$	629.7	443.4
3	$C_{78}H_{104}N_4O_6S^{2+}$	612.5	443.3
4	$C_{78}H_{104}N_4O_7S2^{2+}$	636.4	443.3, 398.3
5	$C_{39}H_{53}N_2O_4S^+$	645.4	443.3, 399.2, 430.3
6	$C_{78}H_{104}N_4O_7S^{2+}$	620.6	443.3, 430.3, 398.2

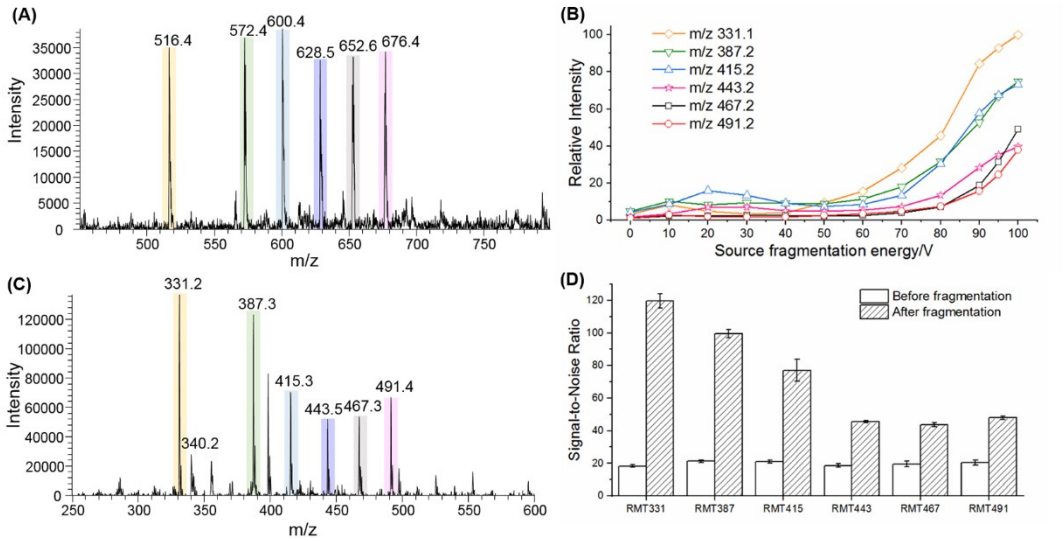

Fig. S8 (A) The mass spectrum of the dissociated six GNP@RMTs before fragmentation (m/z = 516.4, 572.4, 600.4, 628.5, 652.6 and 676.4). (B) The relative intensities of six RMTs and after fragmentation (m/z = 331.1, 387.2, 415.2, 443.2, 467.2 and 491.2) under source fragmentation energy from 0 to 100 V. (C) The mass spectrum of the dissociated six RMTs after fragmentation. (D) The signal-to-noise ratios of representative signals of six RMTs before fragmentation (m/z = 516.4, 572.4, 600.4, 628.5, 652.6 and 676.4) and after fragmentation (m/z = 331.2, 387.3, 415.3, 443.5, 467.3 and 491.4).

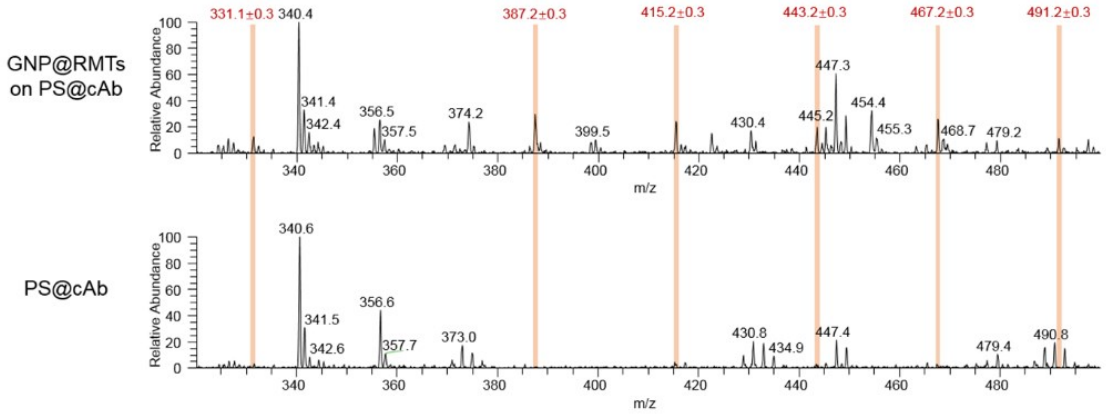

Fig. S9 The mass spectra of the dissociated six GNP@RMTs from paper substrates modified with capture antibodies prepared as immune procedure and blank paper substrates modified with capture antibodies, showing negligible interference of complex immune condition for mass reporter tag readout using relative lower resolution mass spectrometer.

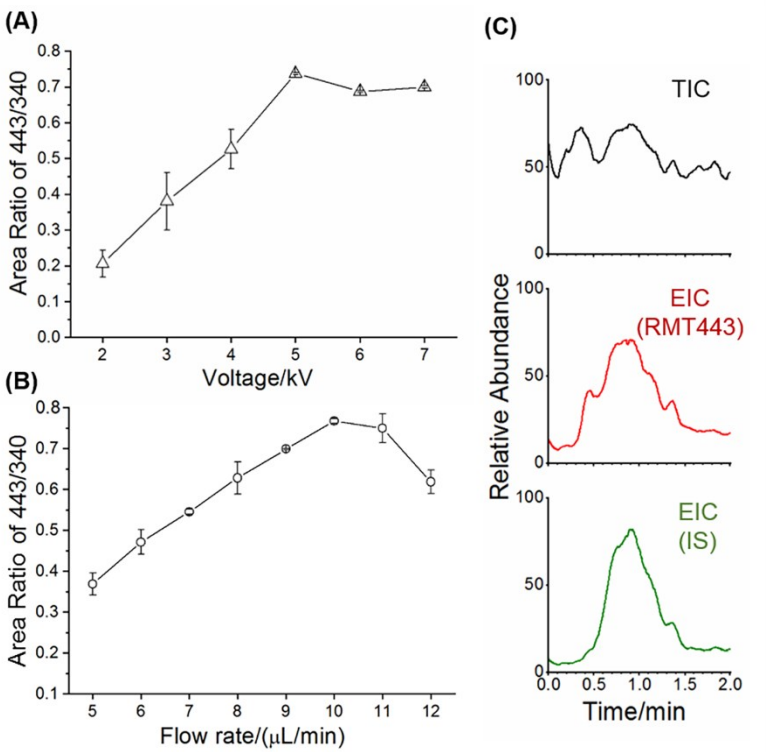

Fig. S10 The optimization of spray voltage (A) and solvent flow rate (B) for the paper substrate-based electrospray ionization MS (PS-ESI MS) system, using the area ratios of the mass reporter of RMT443 (m/z = 443.2) and the fragment of IS (m/z = 340.3) for evaluation. (C) One test sample detected by PS-ESI MS with about 1 min signal duration for RMT443 and IS.

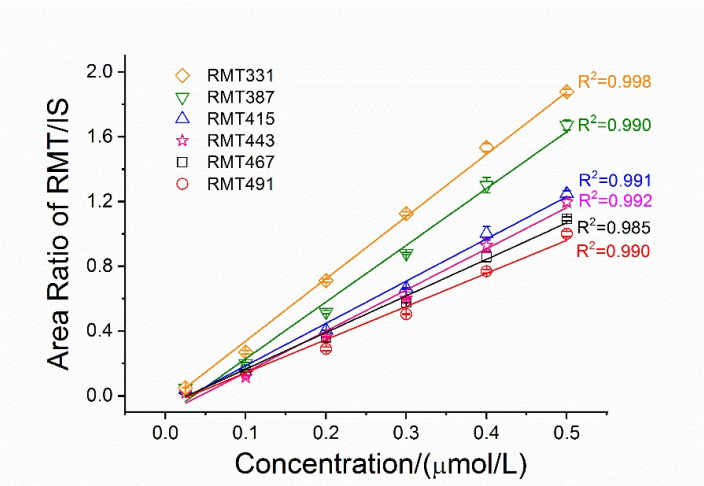

Fig. S11 The calibration curves of the area ratios of six RMT reporters (m/z = 331.1, 387.2, 415.2, 443.2, 467.2 and 491.2) and IS (crystal violet, m/z = 340.2) in different RMT concentrations.

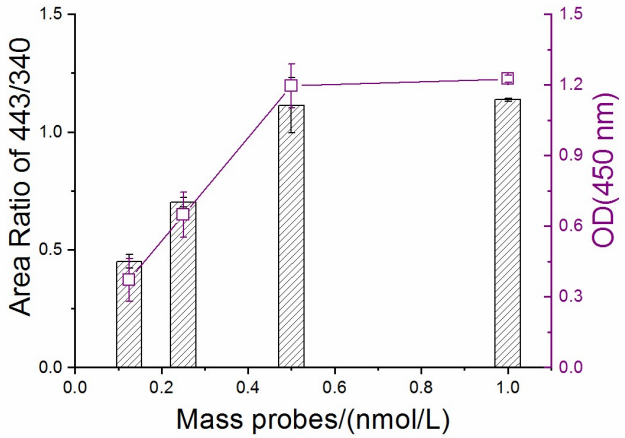

Fig. S12 The optimization of the concentrations (from 0.1 nmol/L to 1 nmol/L) of 40 μL mass probes for the detection of IgG, the 450 nm values and MS signals of RMT443 fragment (m/z = 443.2) and IS (m/z = 340.2) for evaluation.

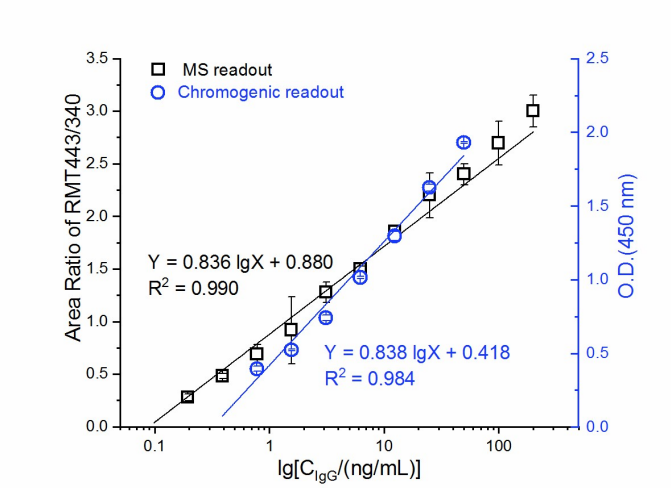

Fig. S13 The calibration curves of MS signal area ratios (RMT443 and IS)/O.D. 450 nm values and logarithm of IgG concentrations in PBS.

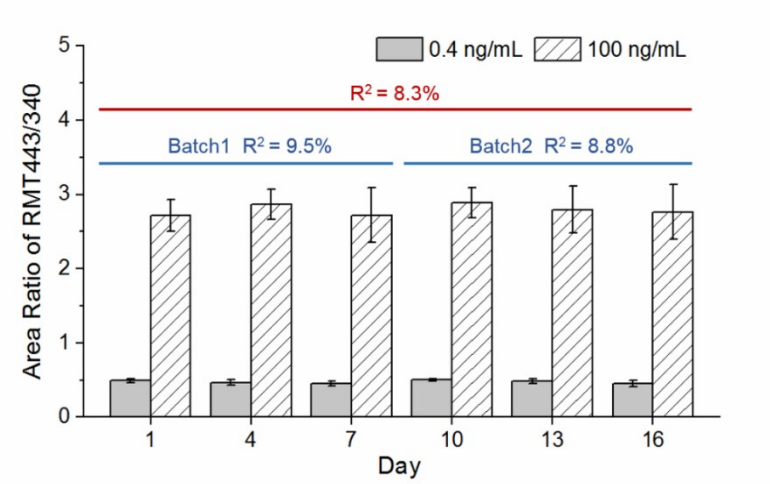

Fig. S14 The robustness validation of the anti-IgG modified paper substrates and GNP@anti-IgG/RMT443 for the detection of IgG with low concentration of 0.4 ng/mL and high concentration of 100 ng/mL. One batch of paper substrates and mass probes were used for three tests on different days after their preparation, and two batches were tested, both showing good repeatability.

Table S3 Calibration curves for CA15-3, CA19-9, CEA, CA125, HE4, and AFP simultaneous detection in PBS buffer by PS-ESI MS and their cut-off values in clinical diagnosis.

Targets	RMTs	Linear equation	Linear ranges	Limits of detection	Cut-off values
CA15-3	RMT331	$Y = 0.0125\ X$/(U/mL) + 0.236 ($R^2 = 0.980$)	1.6-100 U/mL	0.903 U/mL	25 U/mL
CA19-9	RMT387	$Y = 0.00538\ X$/(U/mL) + 0.229 ($R^2 = 0.992$)	1.6-100 U/mL	0.825 U/mL	40 U/mL
CEA	RMT415	$Y = 0.0540\ X$/(ng/mL) + 0.182 ($R^2 = 0.990$)	0.3-10 ng/mL	0.154 ng/mL	5 ng/mL
CA125	RMT443	$Y = 0.00571\ X$/(U/mL) + 0.153 ($R^2 = 0.992$)	3.1-100 U/mL	1.612 U/mL	35 U/mL
HE4	RMT467	$Y = 1.33\ X$/(nmol/L) + 0.219 ($R^2 = 0.987$)	0.016-0.5 nmol/L	0.00830 nmol/L	140 pmol/L
AFP	RMT491	$Y = 0.00172\ X$/(ng/mL) + 0.0300 ($R^2 = 0.998$)	3.1-200 ng/mL	1.56 ng/mL	10 ng/mL

Table S4 Standard addition measurements of CA15-3 with two concentrations and high concentrations of other five protein markers in serum.

	Added	Area ratio	Detected	Recovery%	RSD% (*n*=6-12)
CA15-3/(U/mL)	**10**	**0.363**	**10.1**	**101**	**12**
	50	**0.850**	**49.2**	**98.3**	**4.0**
CA19-9/(U/mL)	100	0.722	91.6	91.6	4.3
CEA/(ng/mL)	10	0.781	11.1	111	7.1
CA125/(U/mL)	100	0.688	93.7	93.7	2.3
HE4/(pmol/L)	0.5	0.886	0.502	100	4.9
AFP/(ng/mL)	200	0.370	197	98.7	11

Table S5 Standard addition measurements of CA19-9 with two concentrations and high concentrations of other five protein markers in serum.

	Added	Area ratio	Detected	Recovery%	RSD% (*n*=6-12)
CA15-3/(U/mL)	100	1.46	97.9	97.9	2.1
CA19-9/(U/mL)	**10**	**0.279**	**9.26**	**92.6**	**3.7**
	50	**0.465**	**43.8**	**87.7**	**5.3**
CEA/(ng/mL)	10	0.762	10.7	107	5.2
CA125/(U/mL)	100	0.669	90.3	90.3	3.5
HE4/(pmol/L)	0.5	0.892	0.506	101	4.0
AFP/(ng/mL)	200	0.386	207	104	6.9

Table S6 Standard addition measurements of CEA with two concentrations and high concentrations of other five protein markers in serum.

	Added	Area ratio	Detected	Recovery%	RSD% (*n*=6-12)
CA15-3/(U/mL)	100	1.47	99.1	99.1	2.2
CA19-9/(U/mL)	100	0.704	88.4	88.4	5.4
CEA/(ng/mL)	**1**	**0.237**	**1.02**	**102**	**13**
	5	**0.465**	**5.25**	**105**	**5.5**
CA125/(U/mL)	100	0.679	92.2	92.2	4.6
HE4/(pmol/L)	0.5	0.877	0.495	99.0	1.2
AFP/(ng/mL)	200	0.371	198	99.2	4.2

Table S7 Standard addition measurements of CA125 with two concentrations and high concentrations of other five protein markers in serum.

	Added	**Area ratio**	**Detected**	**Recovery%**	**RSD% (*n*=6-12)**
CA15-3/(U/mL)	100	1.47	98.5	98.5	2.9
CA19-9/(U/mL)	100	0.702	88.0	88.0	4.5
CEA/(ng/mL)	10	0.751	10.5	105	3.2
CA125/(U/mL)	**10**	**0.217**	**11.3**	**113**	**7.5**
	50	**0.405**	**44.1**	**88.2**	**3.2**
HE4/(pmol/L)	0.5	0.891	0.505	101	1.5
AFP/(ng/mL)	200	0.371	199	99.3	7.3

Table S8 Standard addition measurements of HE4 with two concentrations and high concentrations of other five protein markers in serum.

	Added	**Area ratio**	**Detected**	**Recovery%**	**RSD% (*n*=6-12)**
CA15-3/(U/mL)	100	1.48	99.5	99.5	4.1
CA19-9/(U/mL)	100	0.715	90.2	90.2	2.2
CEA/(ng/mL)	10	0.772	10.9	109	6.1
CA125/(U/mL)	100	0.671	90.7	90.7	6.1
HE4/(pmol/L)	**0.05**	**0.293**	**0.0556**	**111**	**4.1**
	0.25	**0.560**	**0.257**	**103**	**8.9**
AFP/(ng/mL)	200	0.364	194	97.2	3.9

Table S9 Standard addition measurements of AFP with two concentrations and high concentrations of other five protein markers in serum.

	Added	**Area ratio**	**Detected**	**Recovery%**	**RSD% (*n*=6-12)**
CA15-3/(U/mL)	100	1.49	100.0	100	3.5
CA19-9/(U/mL)	100	0.724	91.9	91.9	2.7
CEA/(ng/mL)	10	0.754	10.6	106	7.0
CA125/(U/mL)	100	0.696	95.1	95.1	8.9
HE4/(pmol/L)	0.5	0.884	0.500	100	5.2
AFP/(ng/mL)	**20**	**0.0693**	**22.9**	**114**	**3.7**
	100	**0.204**	**101**	**101**	**1.0**

Table S10 Performances of existing multiplexed immunoassays with simultaneous read-out techniques for cancer biomarker detection in serum.

Methods	Biomarkers	Labeling materials	Sample needed	Time*	Linear ranges	Limits of detection	Ref
ELISA	CEA Cyfra21-1 NSE	MGCB-Ab2-cGO	100 μL	>120 min	20 pg/mL-10 ng/mL 1 pg/mL-10 ng/mL 0.1 pg/mL-10 ng/mL (IgG)	20 pg/mL 1 pg/mL 0.1 pg/mL	S1
FIA (FRET)	NSE SCC CEA Cyfra21-1 CA15-3	Dye-Ab	50 μL	~45 min	-	~ ng/mL	S2
FIA	CEA PSA AFP VEGF	Dye-Ab ribonuclease H	5 μL	>60 min	5 pg/mL–500 ng/mL 2 pg/mL–200 ng/mL 1 pg/mL–100 ng/mL 4 pg/mL–400 ng/mL	2.94 pg/mL 1.25 pg/mL 0.65 pg/mL 2.26 pg/mL	S3
SERS-IA	cTnI NT-ProBNP NGAL	Raman reporter-nanostars-Ab	20 μL	>80 min	1 fg/mL-1 μg/mL	0.76 fg/mL 0.53 fg/mL 0.41 fg/mL	S4
ECLIA	CEA AFP *β*-HCG	Ruthenium(II)/iridium(III) complexes-Ab	300 μL	>180 min	-	5 ng/mL 25 ng/mL 5 mIU/mL	S5
ECLIA	CEA AFP	CdTe-Ab CdSe-Ab	20 μL	>150 min	1 pg/mL-10 ng/mL 10 fg/mL-100 pg/mL	1 pg/mL 10 fg/mL	S6
ICP-MS IA	CEA AFP FER	Ho/Eu/Pr-DNA-Ab	50 μL	>180 min	~0-100 pg/mL	3.31 pg/mL 5.31 pg/mL 2.02 pg/mL	S7

Methods	Biomarkers	Labeling materials	Sample needed	Time*	Linear ranges	Limits of detection	Ref
spICPMS IA	CA125 CEA CA199	AuNPs/AgNPs /PtNPs-Ab	10 μL	>120 min	2-200 U/mL 2-500 ng/mL 1-500 U/mL	0.43 U/mL 0.90 ng/mL 0.80 U/mL	S8
LDI-MS IA	lactoferrin BSA	PEG-GNPs-Ab	3−30 nL	>60 min	-	18 pg/mL 54 pg/mL	S9
PSI-MS IA	malaria *Pf*HRP2 CA125 CEA	ITEA/ITBA-Ab	20 μL	>60 min	0.05-10 nmol/L	2.8 ng/mL 250 U/mL 100 ng/mL	S10
This work	CA15-3 CA19-9 CEA CA125 HE4 AFP	RMTs/Ab-GNPs	10μL	<60 min	1.6-100 U/mL 1.6-100 U/mL 0.3-10 ng/mL 3.1-100 U/mL 0.016-0.5 nmol/L 3.1-200 ng/mL	0.903 U/mL 0.825 U/mL 0.154 ng/mL 1.612 U/mL 0.00830 nmol/L 1.56 ng/mL	

*Time was calculated from the addition of serum sample to the read-out of the results for one test.

ELISA: Enzyme-linked immunosorbent assay; FIA: Fluorescence immunoassay; FRET: Förster resonance energy transfer; SERS-IA: Surface enhanced raman scattering immunoassay; ECLIA: Electrochemiluminescence Immunoassay; ICP-MS IA: Inductively coupled plasma mass spectrometry immunoassay; spICPMS IA: Single-particle inductively coupled plasma mass spectrometry immunoassay; LDI-MS IA: Laser desorption ionization mass spectrometry immunoassay; PSI-MS IA: Paper spray ionization mass spectrometry immunoassay.

Table S11 Detection results of six cancer biomarkers in 12 patient serum sample by PS-ESI MS-based immunoassays and the clinical ECLIA.

	CA153/(U/mL)		CA199/(U/mL)		CA125/(U/mL)		CEA/(ng/mL)		AFP/(ng/mL)	
	ECLIA	**PS-ESI MS (*n* = 6)**	**ECLIA**	**PS-ESI MS (*n* = 6)**	**ECLIA**	**PS-ESI MS (*n* = 6)**	**ECLIA**	**PS-ESI MS (*n* = 6)**	**ECLIA**	**PS-ESI MS (*n* = 6)**
L1	10.8	10.6±0.31	42.1	43.3±0.91	10.4	11.4±0.33	3.45	3.68±0.13	13.9	12.8±0.45
L2	7.64	7.92±0.56	4.55	4.28±0.22	13.9	12.1±0.54	0.640	0.611±0.016	130	128±2.8
L3	*N*	13.2±0.59	10.6	12.8±0.51	7.23	7.88±0.25	3.06	3.20±0.13	88.9	88.4±3.6
B1	11.1	12.0±0.35	18.9	19.3±0.83	24.5	25.7±0.56	0.930	1.04±0.073	1.60	*n*
B2	9.37	9.20±0.20	23.2	23.4±1.6	16.2	17.0±1.0	1.80	1.30±0.12	1.88	*n*
B3	10.8	10.8±0.58	22.9	22.5±1.1	29.9	29.4±1.8	1.27	1.17±0.061	1.97	*n*
B4	5.77	5.20±0.18	10.8	11.1±0.44	10.4	11.7±0.85	0.720	0.722±0.030	3.18	3.49±0.31
B5	7.26	7.12±0.11	9.10	9.48±0.65	7.44	6.83±0.28	0.610	0.667±0.023	1.51	*n*
B6	13.3	14.0±1.8	0.610	*n*	14.2	15.4±1.4	2.15	2.22±0.083	3.15	4.07±0.36
G1	6.77	7.04±0.32	5.09	5.58±0.13	12.9	13.5±0.53	8.81	9.13±0.091	4.22	4.65±0.24
G2	7.31	7.20±0.33	17.0	16.8±0.62	10.4	10.2±0.22	1.54	1.46±0.057	5.74	5.81±0.52
G3	12.4	13.0±0.55	7.83	7.43±0.39	10.2	10.3±0.40	1.84	1.96±0.053	6.56	6.40±0.26
R	**0.993**		**0.998**		**0.990**		**0.997**		**0.999**	

N: Not detected in clinic by ECLIA; n: Out of detection range by PS-ESI MS-based immunoassays; R: Correlation coefficient for the detection results from two different methods.

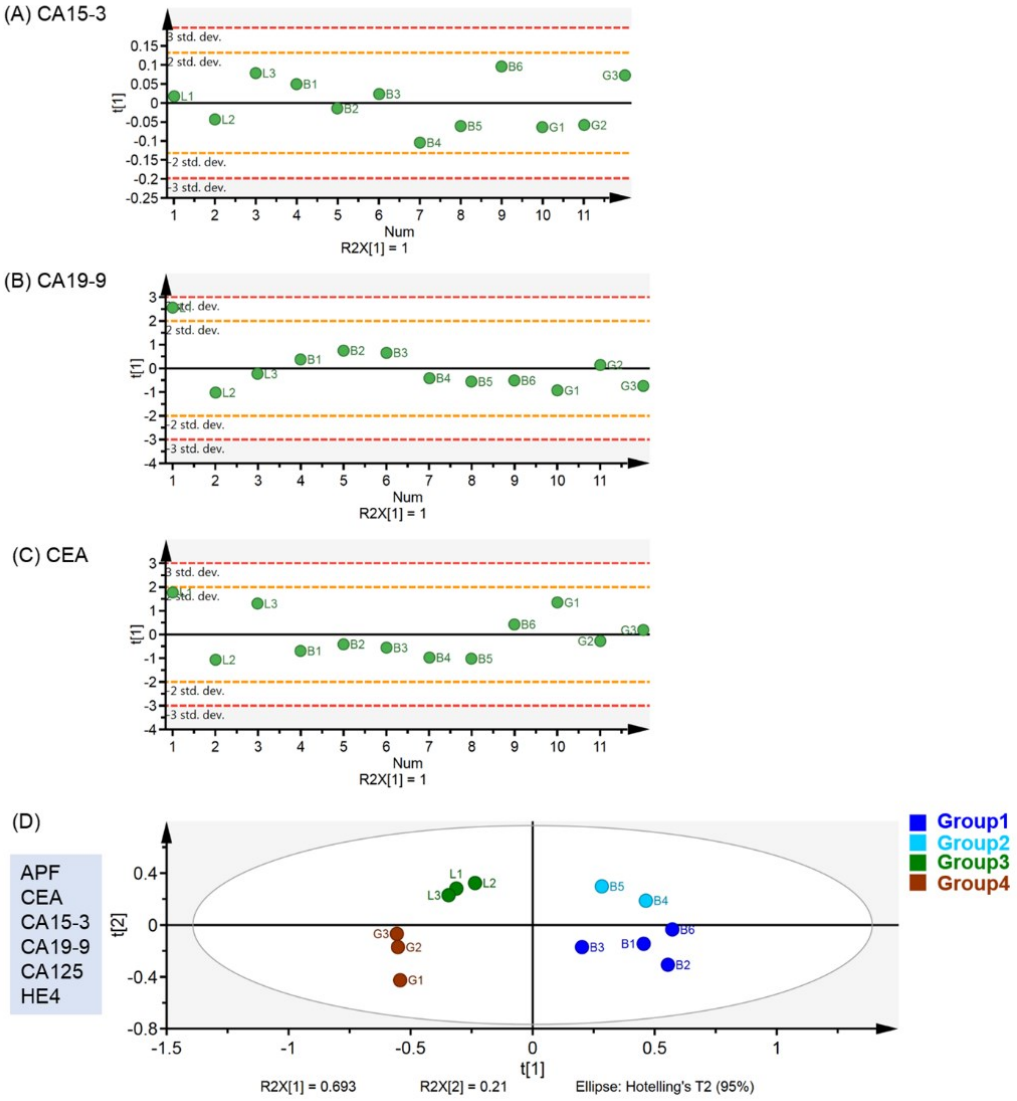

Fig. S15 Principal component analysis (PAC) results (one component) with only one detected calibrated RMT peak areas of biomarkers: (A) RMT331 (CA15-3, known as specific for breast cancer), (B) RMT387 (CA19-9, known as specific for pancreatic cancer), (C) RMT415 (CEA, known as candidate for colorectal cancer, lung cancer, pancreatic cancer, gastric cancer and so on). (D) PCA result of 12 patient serum samples based on the calibrated RMT peak areas of six biomarkers: RMT491 (APF), RMT415 (CEA), RMT331 (CA15-3), RMT387 (CA19-9), RMT443 (CA125) and RMT467 (HE4). Labels of the scatters representing the different tumor series: breast (B1-6), liver (L1-3), and gastric (G1-3), and scatters marked in different four colors based on the results of hierarchical clustering (Ward's method, square Euclidean distance) to four groups. There was the potential for combining six biomarkers to distinguish different sites and even the benign and malignant breast tumors.

References:

S1. C. Li, Y. Yang, D. Wu, T. Li, Y. Yin and G. Li, Chem. Sci., 2016, 7, 3011-3016.

S2. D. Geissler, S. Stufler, H.-G. Loehmannsroeben and N. Hildebrandt, J. Am. Chem. Soc., 2013, 135, 1102-1109.

S3. J. Xu, M. Shi, W. Chen, Y. Huang, L. Fang, L. Yao, S. Zhao, Z.-F. Chen and H. Liang, Chem. Commun., 2018, 54, 2719-2722.

S4. Y. Su, S. Xu, J. Zhang, X. Chen, L.-P. Jiang, T. Zheng and J.-J. Zhu, Anal. Chem., 2019, 91, 864-872.

S5. W. Guo, H. Ding, C. Gu, Y. Liu, X. Jiang, B. Su and Y. Shao, J. Am. Chem. Soc., 2018, 140, 15904-15915.

S6. G. Zou, X. Tan, X. Long, Y. He and W. Miao, Anal. Chem., 2017, 89, 13024-13029.

S7. Z. Hu, G. Sun, W. Jiang, F. Xu, Y. Zhang, M. Xia, X. Pan, Z. Xing, S. Zhang and X. Zhang, Anal. Chem., 2019, 91, 5980-5986.

S8. Z. Huang, Z. Li, M. Jiang, R. Liu and Y. Lv, Anal. Chem., 2020, 92, 16105-16112.

S9. X. Zhong, L. Qiao, N. Gasilova, B. Liu and H. H. Girault, Anal. Chem., 2016, 88, 6184-6189.

S10. S. Chen, Q. Wan and A. K. Badu-Tawiah, J. Am. Chem. Soc., 2016, 138, 6356-6359.